Workspace Control of Two Link Planar Robot Using Micro-Box 2000

Lee Jun Wei*, Ahmad Zaki Hj Shukor, Muhammad Herman Jamaluddin

Center for Robotic and Industrial Automation (CeRIA), Robotic and Industrial Automation (RIA), Faculty of Electrical Engineering, Universiti Teknikal Malaysia Melaka, Durian Tunggal, Malaysia

Graphical abstract

Abstract

This paper presents the workspace/task space control of a two degree of freedom (DOF) two link planar robot manipulator with DC geared motor actuation. Due to the nature of the DC geared motor, PD controller system is designed for each joint of the actuator to minimize the error, improve performance and obtain desired response. This paper includes the modelling of the planar structure and the simulation of workspace control by two methods, inverse kinematics and Direct Cartesian. Then a disturbance compensation called Workspace Observer (WOB) is introduced to improve the Direct Cartesian method. Comparison between the three methods was done. The Direct Cartesian with DOB shows a better trajectory response compared to inverse kinematics.

Keywords: Inverse Kinematics, Direct Cartesian, PD controller, two link open chain manipulator, 2R planar, disturbance observer (DOB), workspace observer (WOB)

1.0 INTRODUCTION

Over the decades, the robotic manipulators have been advancing in technology, for example legged robots, robotic arm and humanoid robots [1]. The technology has been inspired by the biological motion of humans and animals. Some successful developments from this technology include ASIMO, Dexter, DLR robot and others. Moreover, most of these robot configurations are from serial linked configurations, rotary, linear actuation or combinations of both [2]. However, the designs are mostly simplified to obtain results to perform desired task. For example, serial joint servo actuation and gears/mechanism are implemented in industrial robotic manipulators. In addition, many types of manipulator structures apply new studies on kinematics and dynamics [3].

There is a large variant of types of workspace control method. For example, fuzzy logic (an application of artificial intelligence) is able to employ algorithm called self-organizing fuzzy logic estimator to produce joint space at every joint [4]. Another application from artificial intelligent using neural network is applied in solving the inverse kinematic problem [5]. This method follows the procedure of neural network as needed for training phase by calculating the weight of neural networks. This method is effective for avoiding singularity problem. The advantage of this method is that it has the function of setting the angles at joints between maximum and minimum values. This means the end-effector can only reach to any target point in between the set values angles of minimum and maximum values. Computed torque control and feedforward also have been extensively studied in robot manipulators [6]. Rotating coordinate system significantly simplifies the kinematics of a two-link robotic manipulator with the biarticular actuation coordination [7]. As for this paper, the two link open chain manipulator is controlled using Direct Cartesian control scheme which is almost similar with computed-torque control

scheme. The different between these two schemes is that Direct Cartesian is in workspace while computed-torque control is in joint space.

Although the conventional motion control system in the robot industries have improved significantly, the robustness of the manipulators in dealing with internal and external disturbance limit their performance [8]. This means that various types of workspace control method as mentioned above do not have a disturbance eliminator controller inside the system. Thus a disturbance observer (DOB), which is proposed in [9] is included in the system in the workspace control. It is a robust control used to estimate the disturbances and system variation parameters as the key for advanced motion control systems [9], [10]. By using the observers, the robustness and performance of the motion control system are achieved [11].

1.1 Research Focus

In this paper, a two link planar robot manipulator system is controlled in workspace by providing angles (from Inverse Kinematics) to move to desired workspace position. The manipulator is also experimented using Direct Cartesian method with the same workspace trajectory. The objective of this research is to find the difference between different workspace control schemes, inverse kinematic and Direct Cartesian. Furthermore, a comparison is made between the workspace control and implementation of workspace observer (WOB) into the Direct Cartesian system as disturbance compensation.

1.2 Organization of Paper

This paper is organized as follows; Section 2.0 introduces the two links planar robot manipulator, Section 3.0 shows the design of a closed loop control system for a single link manipulator and two link manipulator. Section 4.0 shows the dynamics modelling for inverse kinematics (Method 1) and Direct Cartesian (Method 2) and the implementation of workspace observer (WOB) into the Direct Cartesian system as a disturbance compensation. Section 5.0 discusses experiments and the results of the three methods used.

2.0 TWO LINK PLANAR ROBOT MANIPULATOR

Each joint is actuated by a planetary DC geared motor with Hall Effect incremental encoder. It has 245ppr (pulse per revolution) and also with top speed of 120rpm (revolution per minute). The two links are designed with a 0.12m each with a base attached to a thick aluminum platform to prevent any unwanted vibration. A motor driver is used to control the actuator. By using this motor driver, two separate signals are needed, one for direction (counterclockwise or clockwise) and another for speed of the motor. To control motor direction, HIGH or LOW signal is supplied for different directions, whereas PWM signal is fed to control the motor speed. The PWM signal is generated from PWM Generator which is available from the Simulink library browser, which provide duty cycle signal to the motor driver. Figure 1 shows the two degree-of-freedom (DOF) manipulator in SolidWorks and Figure 2 shows the picture of the manipulator assembled.

Micro-Box 2000 x86 Based Real-Time System is an affordable and robust platform for rapid control prototyping applications as shown in Figure 3. It is rugged, high performance and can fulfil real-time analysis and control system testing needs. The control system for these experiments is designed using Simulink which is integrated to the Micro-Box and allow real-time modeling and simulation of control systems which is important to plot real time data. Moreover, the sampling time of this Micro-Box can go up to 1ms.
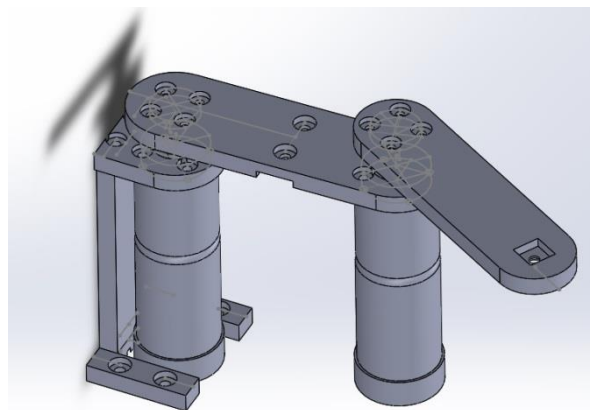
Figure 1 Two DOF Robot Manipulator (SolidWorks model)
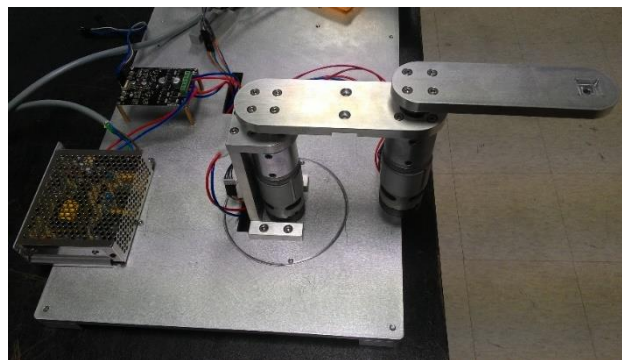
Figure 2 Overall 2DOF Robot Manipulator

Specifications of the Micro-Box:
1. Rugged, high performance industrial PC.
   - Fan less, low-power consumption design (22W typical)
   - Support for all standard PC peripherals, includes external floppy.
   - Sturdy, compact size.
2. I/O-equipped with AD/DA, Encoder, CAN, and DI/O modules.

3. Onboard Celeron® M 1GHz/256 MB DDR RAM, 64MB compact flash RAM (expandable to 1GB).
4. Stand-alone operation with xPC Target Embedded OptionTM. Users can write the Simulink® model onto a CF card without an Internet connection.
5. I/O pins specifications in Figure 4.

Figure 3 Micro-Box 2000 x86 Based Real-Time System

Type	Specification
A/D	8 channels, ±10 volts,16 bits, single-end
D/A	4 channels, ±10 volts ,16 bits,
Encoder	4 channels, 24 bits, 0V/5V, A/B/Index
DIO	16 channels(8 from parallel-port), TTL
CAN	2 ports, CAN2.0b compactable, speed up to1Mbps

Figure 4 Micro-Box 2000 I/O pins

3.0 SINGLE LINK CLOSED LOOP CONTROL SYSTEM

Single link closed loop system is designed and tested for the single link manipulator. To control a motor's position and velocity under varying load conditions, a PD controller system is place in the DC geared motor system or the joint system. The performance of the system is determined by tuning two parameters for the Proportional term, K_p and Derivative terms, K_d. The proportional term is used to set the system response time, or settling time. The shorter the settling time, the better the performance. Moreover, the derivative term is used to prevent the control loop from overshooting the target. The more the overshoot, the more unstable the system becomes. Thus, short settling time and small overshoot is the desired response for the DC geared motor.

Both of these characteristics can be adjusted using natural frequency, ω_n and damping coefficient, δ as shown in (3.1) and (3.2). Equation (3.3) shows the basic PD controller system while (3.4) is the PD controller system applied to each of the joint system. Figure 5 shows the block diagram of a DC geared motor control system from each joint which is a sub-block diagram of a 2 DOF Robotic Arm Manipulator. It consists of a PD controller to keep the error minimum, improve performance and obtain the desired response (critical damping). To get the angular

velocity and angular acceleration, a simple derivative, $\frac{du}{dt}$ is applied.

A PD controller is used because it is simple to tune the gain, and in the later section, WOB is implemented which as a function similar to the integrator (I) but can reject disturbance.

$$K_p = \omega_n^2 \qquad (3.1)$$

$$K_d = 2\delta\omega_n \qquad (3.2)$$

$$u(t) = K_p e(t) + K_d \frac{d}{dt} e(t) \qquad (3.3)$$

$$u(t) = K_{p\theta}\big(\theta_{ref} - \theta\big) + K_{d\theta}\big(\dot{\theta}_{ref} - \dot{\theta}\big) + \ddot{\theta}_{ref} \qquad (3.4)$$
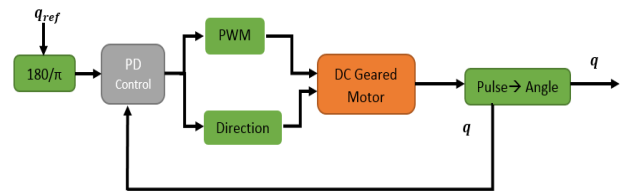
Figure 5 Single Link Close Loop System Block Diagram

Figure 6 shows the responses of the single link system when a step input of angles is fed into the single link closed loop system with and without PD controller. The PD controller makes the settling time faster compared to sluggish response without PD controller. The responses are desired responses with short settling time and small overshoot.
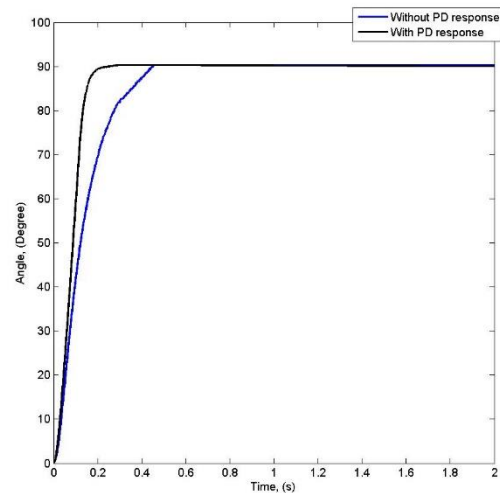
Figure 6 Step input of angle 90˚

3.1 Two Links Closed Loop Control System

Two links closed loop system is designed and tested for both joints of actuators with two links attached as shown in Figure 2. The PD controller system is implemented to both actuators (at the joints). A few XY position references are given to test the ability of the manipulator to do position tracking. The step input

of XY position is fed into the inverse kinematics to convert XY position axis to reference angles at each joint.
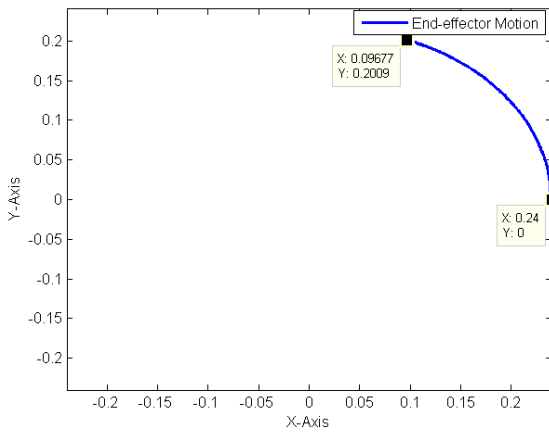
Figure 7 Step input of XY position axis at (0.1, 0.2)
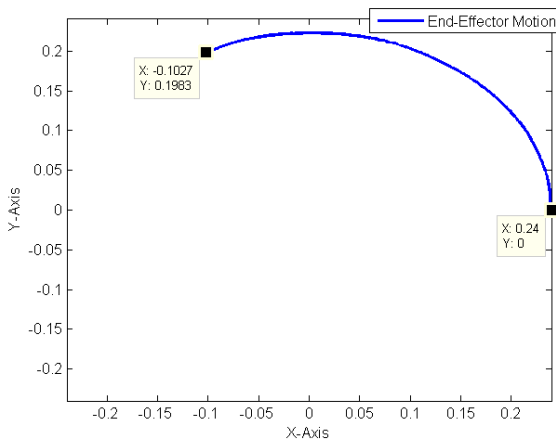
Figure 8 Step input of XY position axis at (-0.1, 0.2)
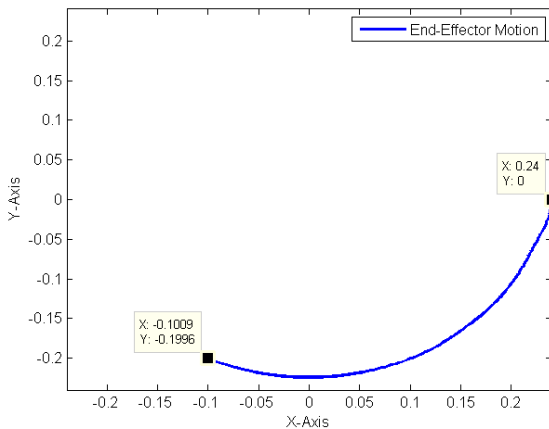
Figure 9 Step input of XY position axis at (-0.1, -0.2)
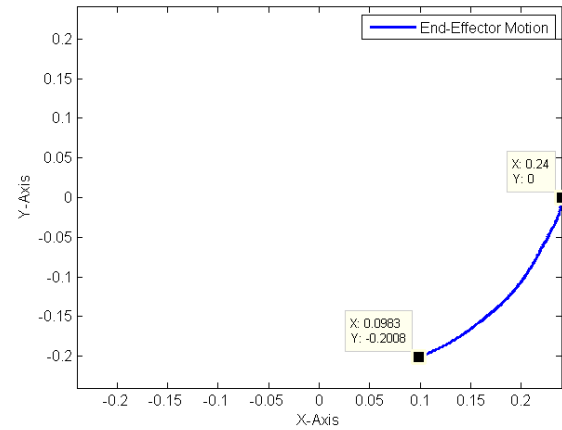
Figure 10 Step input of XY position axis at (0.1, -0.2)

The end effector starts from an XY initial position (0.24, 0), and moves to an XY position target at each quadrant. This is shown in Figures 7 to Figure 10. The results of these figures show the success of the Inverse Kinematics in providing the joint angle references that correspond to workspace reference positions.

4.0 WORKSPACE/TASKSPACE POSITION CONTROL

There are many researches on control of robotic manipulators. Some of many examples are torque sensorless control [12], feedforward and computed torque control [13], SCARA manipulator tracking control [14], and position control of constrained robotic system [15]. In [1], a control method of an interesting actuator, the spiral motor was investigated. The spiral motor is a good prospect for control of musculoskeletal structure. In this paper, we present the inverse kinematics approach and the Direct Cartesian approach for the general structure of a two link open chain planar robot manipulators system.

Consider a workspace/task space circular reference trajectory that the end effector has to follow. The references for the x and y axis position are denoted by the (4.1) (0.044, 0.06 are x, y positions of the center of the circle);

$$x(t) = 0.044\cos\omega(t) + 0.18;$$

$$y(t) = 0.06\sin\omega(t) + 0.06;$$

$$\omega(t) = 2\pi(1 - \cos(t)); \qquad (4.1)$$

For workspace control of the reference trajectories, three methods were implemented. Table 1 shows the three types of methods propose and present the comparision between this three methods.

Table 1 Control Methods

Method 1	Inverse Kinematics + PD on both actuator
Method 2	Direct Cartesian
Method 3	Direct Cartesian + WOB on both actuator

4.1 Dynamics Modelling

4.1.1 Method 1 (Inverse Kinematics + PD on both actuator Approach)

For a two link planar rotary manipulator, the joint space coordinates can be obtained from (4.2). These joint space trajectories are obtained from the Cartesian reference trajectories $(x, y$ are workspace/taskspace coordinates). The reference angles are then fed to the PD controller. The control of each joint is independent of each other.

$$D = \frac{x^2 + y^2 - l_1^2 - l_2^2}{2l_1l_2}$$

$$\theta_1 = tan^{-1}\sqrt{\frac{(1 - D^2)}{D}}$$

$$\theta_2 = tan^{-1}\frac{y}{x} - tan^{-1}\frac{l_1 sin\theta_2}{l_1 + l_2 cos\theta_2}$$

$$(4.2)$$

The block diagram of Method 1 (Inverse Kinematics) is shown in Figure 11.
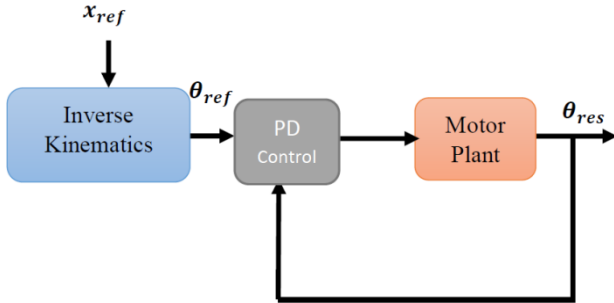
Figure 11 Block Diagram of Method 1

4.1.2 Method 2 (Direct Cartesian + PD on both Actuator Approach)

There are many researches that investigate control of 2R manipulators [16]. In the paper mentioned, the modelling of unconstrained open-chain manipulators used Ordinary Differential Equations via Newton-Euler dynamics algorithm.

Equation (4.3) is the computed closed-form dynamic equation for the two-link planar manipulator shown in Figure 2. The length of the links are labeled as l_1 and l_2. For simplicity, the mass distribution is simple, as assumed all mass existed as a point mass at the distal end of each link. These masses are m_1 and m_2. This dynamic equation is developed in terms of the position and time derivatives of the manipulator joint

angles, or in joint space which are θ_1 and θ_2. The subscript $_1$ and $_2$ are referred to joint or link 1 and joint 2 or link 2 respectively. As this equation also give expressions for the torque at each actuator as a function of joint position, velocity and acceleration (with M as inertia/mass, V as Centrifugal/Coriolis and τ torques/forces);

$$\tau = M(\theta)\ddot{\theta} + V(\theta, \dot{\theta})\dot{\theta} + g(\theta)\theta \qquad (4.3)$$

Equation [4.4] defines the manipulator mass matrix, $M(\theta)$. It is composed of all terms which multiply $\ddot{\theta}$ and is a function of θ;

$$M(\theta) = \begin{bmatrix} m_{11} & m_{12} \\ m_{21} & m_{22} \end{bmatrix} \qquad (4.4)$$

where;

$$m_{11} = l_2^2 m_2 + 2l_1 l_2 m_2 cos(\theta_2) + (m_1 + m_2)$$

$$m_{12} = l_2^2 m_2 + l_1 l_2 m_2 cos(\theta_2)$$

$$m_{21} = l_2^2 m_2 + l_1 l_2 m_2 cos(\theta_2)$$

$$m_{22} = l_2^2 m_2$$

The velocity term, $V(\theta, \dot{\theta})$, shown in Equation [4.5] contains all those term that have any dependence on joint velocity;

$$V(\theta, \dot{\theta}) =$$

$$\begin{bmatrix} -m_2 l_1 l_2 sin(\theta_2)\dot{\theta}_2^2 - 2l_1 l_2 m_2 sin(\theta_2)\dot{\theta}_1 \dot{\theta}_2 \\ m_2 l_1 l_2 sin(\theta_2)\dot{\theta}_1^2 \end{bmatrix} \qquad (4.5)$$

where $-m_2 l_1 l_2 sin(\theta_2)\dot{\theta}_2^2$ is caused by Centrifugal force and $-2l_1 l_2 m_2 sin(\theta_2)\dot{\theta}_1 \dot{\theta}_2$ is caused by a Coriolis force. But in this experimental setup, the g as gravity term is considered negligible and the setup is intended to be in SCARA configuration.

While in the inverse kinematics, $M(\theta)$, $V(\theta, \dot{\theta})$ and $g(\theta)$ term are not inserted in the control. However, the Direct Cartesian used these terms to construct forward kinematic, PD workspace control terms and Jacobians.

Rather than just maintaining the end effector at a desired location, trajectory-following control is used so that the end effector can be made to follow a changing trajectory. The trajectory is given by a function of time that specifies the desired position of the end effector. The trajectory-following control is as shown in (4.6);

$$A = K_{px}(x_{ref} - x_{res}) + K_{dx}(\dot{x}_{ref} - \dot{x}_{res}) + \ddot{x}_{ref}$$

$$B = K_{py}(y_{ref} - y_{res}) + K_{dy}(\dot{y}_{ref} - \dot{y}_{res}) + \ddot{y}_{ref} \qquad (4.6)$$

The subscript $_{ref}$ and $_{res}$ are referred to reference and response respectively. Equation (4.7) relates the

joint torque, τ at the actuator and the fictitious forces, F_{ref} acting on the end effector;

$$\tau = {}^{\circ}J_{aco}{}^{T} F_{ref} \qquad (4.7)$$

while F_{ref} is derived as below;

$$F_{ref} = Mx \begin{bmatrix} A \\ B \end{bmatrix} \qquad (4.8)$$

where M_x is Cartesian mass matrix equation in Cartesian space;

$$M_x = {}^{\circ}J^{-T} M_{\theta} {}^{\circ}J^{-1} \qquad (4.9)$$

and $J_{aco}{}^{T}$ is transpose of Jacobian matrix equation. Jacobian matrix from the workspace/task space to joint space and contains the following elements;

$${}^{\circ}J_{aco} =$$
$$\begin{bmatrix} -l_1 \sin(\theta_1) - l_2 sin(\theta_1 + \theta_2) & -l_2 sin(\theta_1 + \theta_2) \\ l_1 \cos(\theta_1) + l_2 cos(\theta_1 + \theta_2) & l_2 cos(\theta_1 + \theta_2) \end{bmatrix} \qquad (4.10)$$

$$\tau = K_{tn} I_{ref} \qquad (4.11)$$

where K_{tn} is nominal torque constant.

The I_{ref} is then send to the DC geared motor encoder to turn to the desired angle.

To obtain the workspace XY trajectory from the two link planar robot, the angles obtained from each joint of encoder is converted to workspace XY trajectory by forward kinematics equations as shown in (4.12) (x and y are Cartesian coordinates):

$$x = l_1 \cos(\theta_1) + l_2 cos(\theta_1 + \theta_2)$$
$$y = l_1 \sin(\theta_1) + l_2 sin(\theta_1 + \theta_2) \qquad (4.12)$$

While the speed of end effector with respect to x and y position axis can be obtained by Equation (4.13):

$$\begin{bmatrix} \dot{x} \\ \dot{y} \end{bmatrix} = {}^{\circ}J_{aco} \begin{bmatrix} \dot{\theta}_1 \\ \dot{\theta}_2 \end{bmatrix} \qquad (4.13)$$
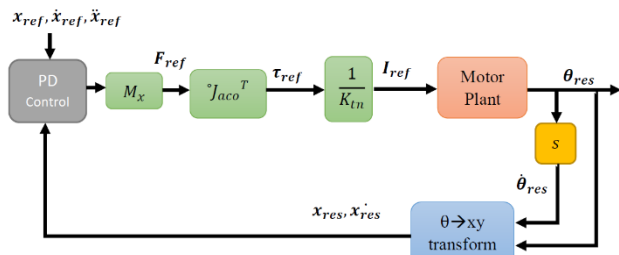
Figure 12 Block Diagram Method 2

The block diagram of Method 2 (Direct Cartesian) is shown in Figure 12.

The equation relating end effector force and joint torque for a two link planar rotary manipulator is derived from Equation [4.14] and [4.15]. Equation [4.15] shows the control law ($\ddot{x}$, $(x_{ref} - x_{res})$, $(\dot{x}_{ref} - x_{res})$, $J_{aco}{}^{T}$, and M_{θ} are Cartesian acceleration, Cartesian error, derivative Cartesian error, transpose Jacobian and Mass matrix, respectively) [17].

$$F_{ref} =$$
$$M_{\theta}(Kp_x(x_{ref} - x_{res}) + Kd_x(\dot{x}_{ref} - \dot{x}_{res}) + \ddot{x}_{ref}) \qquad (4.14)$$
$$\tau =$$
$$J_{aco}{}^{T} M_{\theta}(Kp_x(x_{ref} - x) + Kd_x(\dot{x}_{ref} - \dot{x}) + \ddot{x}_{ref}) \qquad (4.15)$$

Since it is desired that none of the joints overshoot the commanded position or the response be critically damped, the choice of the gain for Kp_x and Kd_x from (4.14) must satisfy the condition of (4.16) and (4.17) where ω_n is natural frequency and δ is damping coefficient.

$$Kp_x = \omega_n^2 \qquad (4.16)$$

$$Kd_x = 2\delta\omega_n \qquad (4.17)$$

4.1.3 Method 3 (Direct Cartesian + WOB on both actuator Approach)
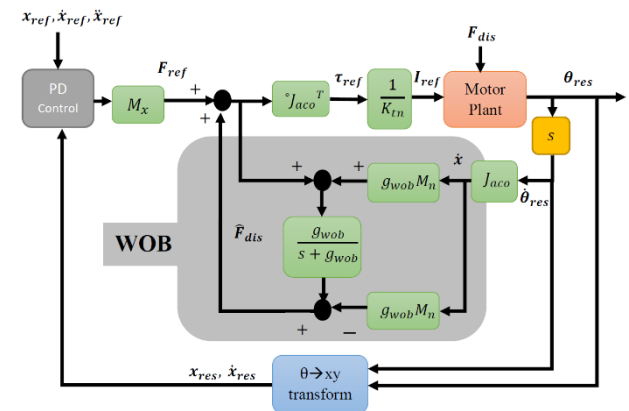
Figure 13 Block Diagram Method 3

In paper [9], the disturbance observer (DOB) is used to estimate the load torque of a motor. Disturbance observer (DOB) is designed to cancel the disturbance torque as quickly as possible. DOB can observe external torque without force sensor. Robust motion control is attained by using the disturbance observer, the robust motion controller makes a motion system to be an acceleration control system. DOB act as disturbance compensation in a motion control system. The output of DOB is only the friction effect under the constant angular velocity motion in the mechanism. DOB is implemented in order to establish robust acceleration controller [10]. A robust system means that the system is insensitive to the external disturbance and parameter variations. It can obtain

wider bandwidth than force sensor due to settling sampling time and observer gain by using DOB [12].

By using this Direct Cartesian method, a PD controller is used because the DOB acts as an integrator, (I). The feedback of estimated disturbance in the inner-loop is to obtain the robustness of the motion control system [18]. Moreover, the PD controller, is designed in outer-loop so that the performance requirements of the motion control system are satisfied [18]. The main advantage of DOB is that the outer-loop can be designed independently controlled without considering the robustness problems of a system [18]. This kind of structure is a two degree of freedom control [10].

However, DOB and WOB is much alike in the sense of structure and function. Workspace observer is built in Cartesian space to compensate the workspace disturbance effect. Workspace observer (WOB) is also able to provide robustness to the system. The principal is similar to disturbance observer (DOB) which is designed in joint space except all values are transposed into force dimension instead of acceleration dimension. Figure 13 shows the Direct Cartesian scheme with workspace observer to compensate the disturbance effect within the motor plant. The estimated force, $\hat{F}_{dis}$ is estimated using (4.20), where M_n is nominal mass.

$$F = F_{ref} - F_{dis} \qquad (4.18)$$

$$F_{dis} = F_{int} + F + D\dot{\theta}_{res} \qquad (4.19)$$

$$\hat{F}_{dis} = \frac{g_{wob}}{s + g_{wob}}(g_{wob}M_n\dot{x} + F) - g_{wob}M_n\dot{x} \qquad (4.20)$$

F_{dis} is the total disturbance force generated in the joint friction and generated in workspace where;

F_{int} Internal force;
F Coulomb friction;
$D\dot{\theta}_{res}$ Viscous force;

$$\frac{g_{wob}}{s + g_{wob}} \qquad (4.21)$$

By using (4.21) the workspace observer is designed to estimate the disturbance force through a low-pass filter, where g_{wob} is a cut-off frequency. The subscript $_{wob}$ and $_{dis}$ are referred to as workspace observer and disturbance respectively.

5.0 EXPERIMENTAL RESULTS AND DISCUSSION

For this setup, (0.224, 0.06) is the initial position of the end effector given to the two links planar robotic arm, the first joint (shoulder) given 0 radians while second joint (elbow) given 0.524 radians. This is also to avoid any unnecessary singularity problem in the computations. After the first one second, the two links planar robotic arm start the trajectories.

The experiments are conducted with the parameters shown in Table 2.

Table 2 Parameters in Experiment

Parameter	Description	Value
l_1	Link 1	0.12m
l_2	Link 2	0.12m
m_1	Mass 1	0.1kg
m_2	Mass 2	0.1kg
K_{tn}	Nominal Torque Constant	0.01595Nm/A
K_p	Proportional gain	6000
K_d	Derivative gain	10
g_{wob}	Cut-off frequency of workspace observer	20rad/s
M_n	Nominal Mass	0.1kg

Figure 2 shows the experimental setup equipment. The workspace circle trajectory of the reference and experiment response of three methods are shown in Figure 14 to Figure 16. The workspace XY trajectory for reference and experimental response for three methods are shown in Figure 17 to Figure 19. Based on Figure 20 to Figure 22, the error between the reference and experimental response of workspace XY position are shown.
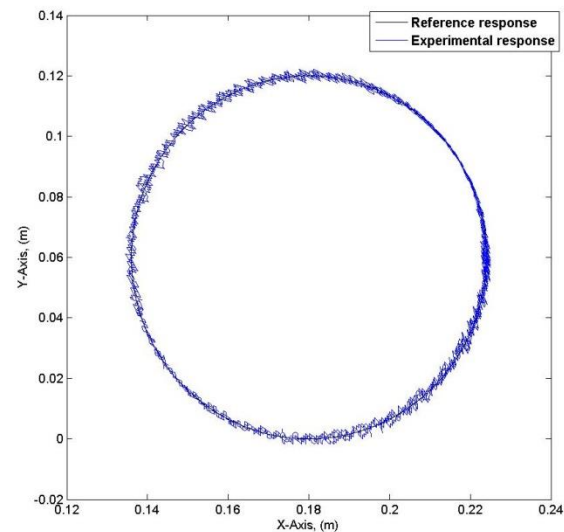
Figure 14 Workspace trajectory of Method 1
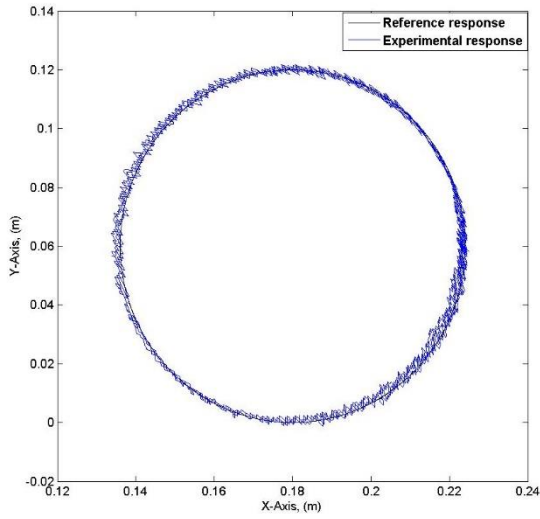
Figure 15 Workspace XY trajectory of Method 2
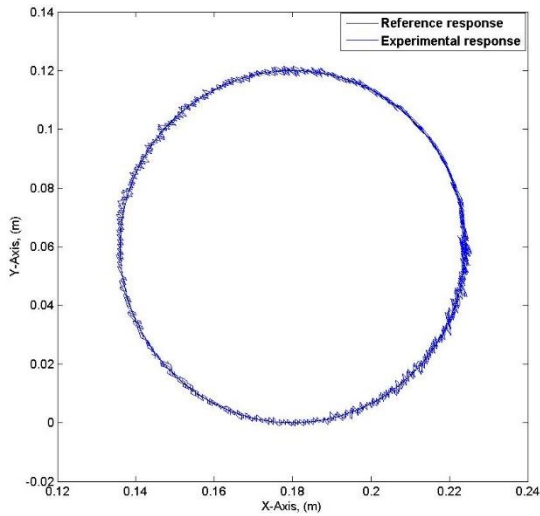
Figure 16 Workspace XY trajectory of Method 3
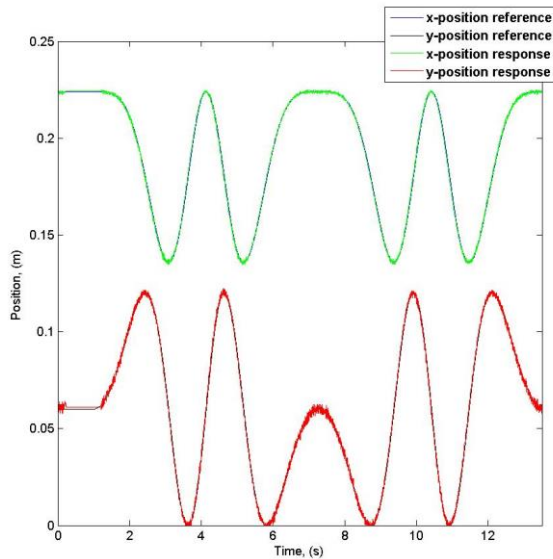
Figure 17 Workspace XY position trajectory of Method 1
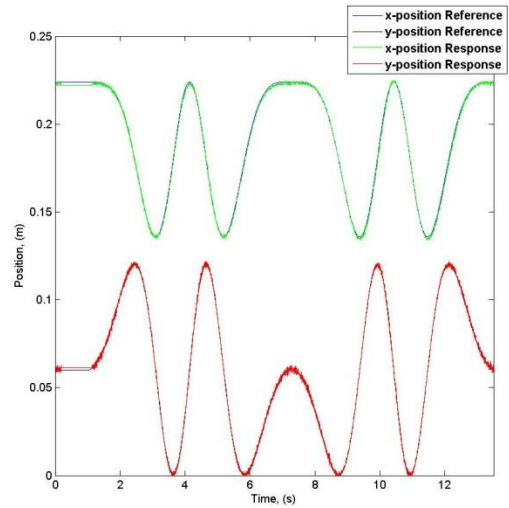
Figure 18 Workspace XY position trajectory of Method 2
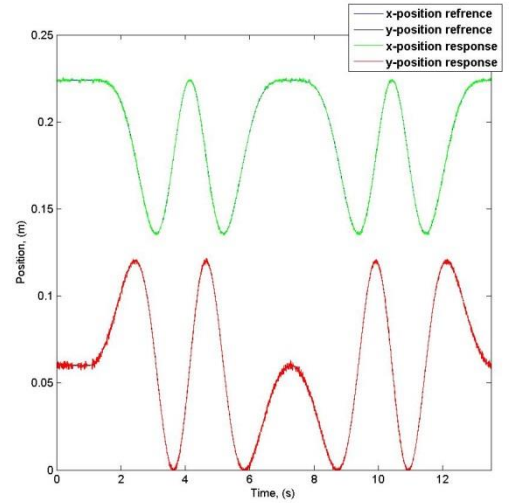
Figure 19 Workspace XY position trajectory of Method 3
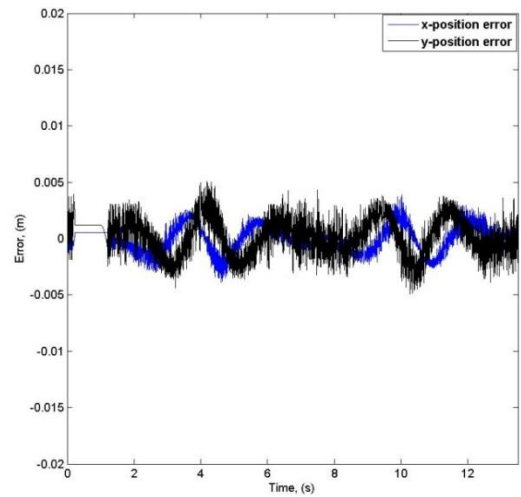
Figure 20 Error in workspace XY position trajectory of Method 1
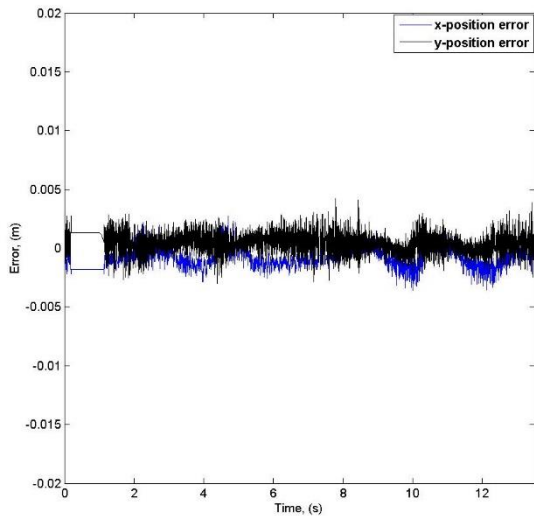
Figure 21 Error in workspace XY position trajectory of Method 2
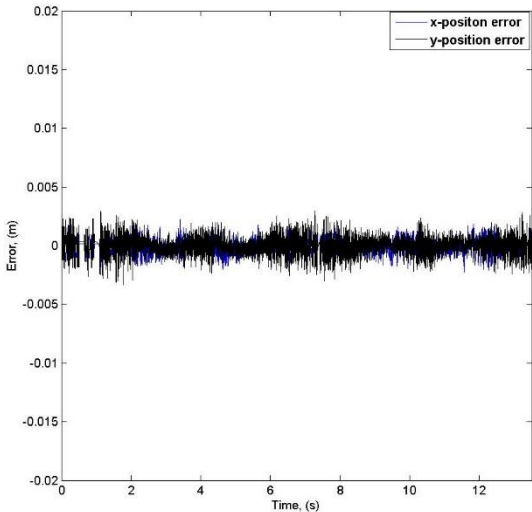
Figure 22 Error in workspace XY position trajectory of Method 3

Table 3 show some comparison parameters between the 3 methods. The three methods for position control in the workspace/task space domain provide some interesting results. It is clear that the inverse kinematics approach and the Direct Cartesian approach yield acceptable responses. Both workspace give almost similar result at the reference as in Figure 14 and Figure 15. Moreover, in terms of error in workspace trajectory, Figure 18 in Method 2 also shows lower error than Figure 17 in Method 1. This proved that Method 2 is a better workspace control method than Method 1.

Although Method 2 uses more computational effort than inverse kinematics, Jacobian in Method 2 generated better joint space trajectory than simple inverse kinematics. Overall, the workspace XY

trajectory for Method 2 Figure 14 shows better trajectory than Method 1 Figure 15.

However, when it comes to comparison between the workspace observer (WOB) at each actuator in Direct Cartesian scheme, the WOB give better standard deviation in x and y position. It improved the overall workspace circle trajectory. In this method, the control using the disturbance observer shows that the bandwidth of force sensing of the reaction torque is wider than the force sensor as mentioned above. When the system is implemented with workspace observer (WOB), the system improved its performance. The x-position and y-position error decreases as the disturbance of the system such as internal force, load force has been removed.

Table 3 Error Comparison (m) between Control Method

Parameters	Method 1	Method 2	Method 3
x_{err}	0.00053	0.000618	$5.9284x10^{-5}$
y_{err}	-0.00021	-0.00036	$2.0219x10^{-5}$
x_{std}	0.001173	0.000798	0.000545
y_{std}	0.001693	0.000878	0.0008299

The workspace XY trajectory result for all three methods have noisy responses. This occurs from the encoder. The encoder on this DC geared motor is just 980 ppr (pulse per revolution) (after 4 times encoding), the derivative of this encoder position generates noise to the signals, even with Low pass filters.

Nevertheless, the slow sampling time can affect the performance of the system [13]. The sampling time of MicroBox is 1ms. Few researches using Field Programmable Gate Array (FPGA) to improve the performance in high computational control system [19]-[21]. In order to achieve high performance, the control algorithm has to be robust, stable, and fast (high control rate). Thus a high computational speed and parallel data processing is needed [20]. Moreover, the sampling rate is inversely proportional to the cut off frequency of a low pass filter used in the disturbance observer (DOB) [21]. The shorter the sampling period, the higher the performance of the system.

6.0 CONCLUSION

This paper presented the modelling and workspace control of the two link planar open chain robot manipulator system. This two DOF consists of incremental encoder embedded on the DC geared motor at both joints. In the simulation, the workspace XY trajectory is controlled by three methods, inverse kinematics, Direct Cartesian and Direct Cartesian with disturbance observer (DOB). Results show that Method 3 (Direct Cartesian with DOB) workspace control is better than the other 2 methods without disturbance compensation.

However, in this paper, the motor mass and the nominal mass parameters are fixed with constant value. These parameters are important when implementing the WOB which will affect the overall robustness and performance of the motion control system. To identify the exact parameters is another heavy scope, but this paper is to show the implementation of WOB which is able to improve the workspace control. More limitations such as low end encoder motor used affect the overall performance of the results

In future, Method 3 will be further implemented to bilateral telerobotic haptic system. The haptic system will implement a reaction force observer to estimate the force from the environment in the bilateral system.

Acknowledgement

References

[1] Shukor, A. Z., Smadi, I. A., Fujimoto, Y. 2011. Development of a Biarticular Manipulator using Spiral Motors. *37th Annual Conference on IEEE, Industial Electronics Society.* 92-97.

[2] Shukor, A. Z., Fujimoto, Y. 2011. Workspace Control of Biarticular Manipulator. *The IEEE Int. Conf. on Mechatronics.* 415-420.

[3] K. Liu, J. M. Fitzgerald, F. L. Lewis. 1993. Kinematics Analysis of a Stewart Platform Manipulator. *IEEE Transactions on Industrial Electronics.* 40(2): 282-293.

[4] Pate, B., Langari Gholamreza. 1993. A Fuzzy Logic Based Controller for a Three Link Manipulator. *Industrial Fuzzy Control and Intelligent Systems.* 109-114.

[5] Yahya, S., Mohamed, H. A. F., M. Moghavvemi, Yang, S. S. 2009. Inverse Kinematics of an Equal Length Links Planar Hyper Redundant Manipulator using Neural Network. ICROS-SICE Internation Joint Conference. 4530-4535.

[6] C. H. An, C. G. Atkeson, J. D. Griffiths, J. M. Hollerbach. 1989. Experimental Evaluation of Feedforward and Computed

[7] Oh, S., Kong Kyoungchul. 2015. Two-Degree-of-Freedom Control of a Two-Link Manipulator in the Rotating Coordinate System. *IEEE Transactions on Industrial Electronics.*

[8] Sabanovic, A., Ohinishi, K. 2011. *Advance Motion Control.* John Wile & Sons.

[9] Ohishi, K. Ohnishi, K., Miyachi, K. 1983. Torque-speed Regulation of DC Motor Based on Load Torque Estimation. In *Proc. IEEJ IPEC-TOKYO.* 2: 1209-1216.

[10] Ohnishi, K., Shibata, M., Murakami, T. 1996. Motion Control for Advanced Mechatronics. *IEEE/ASME Trans. Mechatronics.* 1(1): 56-67.

[11] Sariyildiz, E., Ohnishi, K. 2015. Stability and Robustness of Control Systems. IEEE Transactions on Industrial Electronics. 62(1).

[12] Murakami, T., Yu, F., Ohinishi, K. 1993. Torque Sensorless Control in Multidegree-of-Freedom Manipulator. *IEEE Transactions on Industrial Electronics.* 40(2): 259-265.

[13] An, C. H., Atkeson, C. G., Griffiths, J. D., Hollerbach, J. M. 1989. Experimental Evaluation of Feedforwad and Computed Torque Control. *IEEE Transactions on Robotic and Automation.* 5(3): 368-373.

[14] Visioli, A., Lednani, G. 2002. On the Trajectory Tracking Control of Industrial SCARA Robot Manipulators. *IEEE Transactions on Industrial Electronics.* 49(1): 224-232.

[15] Zhang, Y. X., Chong, S., Shang, W. W., Li, Z. X., Jiang, S. L. 2007. Modelling, Identification and Control of a Redundant Planar 2-DOF Parallel Manipulator. *Int. Journal of Control, Automation and Systems.* 5(5): 559-569.

[16] Shukor, A. Z., Fujimoto, Y. 2012. Planar Task Space Control of a Biarticular Manipulator Driven by Spiral Motors. *International Journal of Advanced Robotics Systems.* 9.

[17] M. W. Spong, M. Vidyasagar. 1989. *Robot Dynamics and Control.* John Wiley and Sons. 23-24.

[18] Sariyildiz, E., Ohnishi, K. 2013. Robust Force Control via Disturbance Observer. *IECON Proceedings (industrial Electronics Conference).* 6551-6556.

[19] E. Ishii, H. Nishi, K. Ohnishi, K. Ohnishi. 2007. Improvement of Performance in Bilateral Teleoperation by Using FPGA. *IEEE Transactions on Industrial Electronics.* 54(4): 1876-1884.

[20] M. Franc, A. Hace. 2012. FPGA Implementation of Performance in Bilateral Teleoperation by Using FPGA. The *12th IEEE International Workshop on Advanced Motion Control.*

[21] H. Tanaka, K. Ohnishi, H. Nishi, T. Kawai, Y. Morikawa, M. Kitajima, S. Ozawa, T. Furukawa. 2007. Bilateral Control in Multi DOF Haptic Surgical Robotic System Utilizing FPGA. *IEEE International Symposium on Industrial Electronics.* 3084-3089.